User-Appropriate Tyre-Modelling
for Vehicle Dynamics in
Standard and Limit Situations

Dr.techn. Wolfgang Hirschberg[*],
Prof. Dr.-Ing. Georg Rill[†],
Dipl.-Ing. Heinz Weinfurter[‡]

SUMMARY

When modelling vehicles for the vehicle dynamic simulation, special attention must be paid to the modelling of tyre-forces and -torques, according to their dominant influence on the results. This task is not only about sufficiently exact representation of the effective forces but also about user-friendly and practical relevant applicability, especially when the experimental tyre-input-data is incomplete or missing.

This text firstly describes the basics of the vehicle dynamic tyre model, conceived to be a physically based, semi-empirical model for application in connection with multi-body-systems (MBS). On the basis of tyres for a passenger car and a heavy truck the simulated steady state tyre characteristics are shown together and compared with the underlying experimental values.

In the following text the possibility to link the tyre model TMeasy to any MBS-program is described, as far as it supports the "Standard Tyre Interface" (STI). As an example, the simulated and experimental data of a heavy truck doing a standardized driving manoeuvre are compared.

1   INTRODUCTION

For the dynamic simulation of on-road vehicles, the model-element "tyre/road" is of special importance, according to its influence on the achievable results. It can be said that the sufficient description of the interactions between tyre and road is one of the most important tasks of vehicle modelling, because all the other components of the chassis influence the vehicle dynamic properties via the tyre contact forces and torques. Therefore, in the interest of balanced modelling,

---

[*]Corresponding Author: Ingenieurbüro Hirschberg, St.Ulrich/Steyr, Austria
[†]FH Regensburg, University of Applied Sciences, Regensburg, FRG
[‡]Ingenieurbüro Hirschberg, St.Ulrich/Steyr

the precision of the complete vehicle model should stand in reasonable relation to the performance of the applied tyre model.

Comparatively lean tyre models are suitable for vehicle dynamics simulations, while, with the exception of some elastic partial structures such as twist-beam axles in cars or the vehicle frame in trucks, the elements of the vehicle structure can be seen as rigid. On the tyres' side, physically based, "semi-empirical" tyre models are proving their worth, where the description of forces and torques relies also on measured and observed force-slip characteristics in contrast to the purely physically founded tyre models. The former class of tyre models, to which the followingly treated tyre model TMeasy belongs, is characterized by an useful compromise between user-friendliness, model-complexity and efficiency in computation time on the one hand, and precision in representation on the other hand.

In vehicle dynamic practice often there exists the problem of data availability for a special type of tyre for the examined vehicle. Considerable amounts of experimental data for car tyres has been published or can be obtained from the tyre manufacturers. If one cannot find data for a special tyre, its characteristics can be estimated at least by an engineer's interpolation of similar tyre types. In the field of truck tyres there is still a considerable backlog in data provision. These circumstances must be respected in conceiving a user-friendly tyre model.

For a special type of tyre, usually the following sets of experimental data are provided:

- longitudinal force versus longitudinal slip (mostly just brake-force),

- lateral force versus slip angle,

- aligning torque versus slip angle,

- radial and axial compliance characteristics,

whereas additional measurement data under camber and low road adhesion are rather favourable special cases.

Any other correlations, especially the combined forces and torques, effective under operating conditions, often have to be generated by appropriate assumptions with the model itself, due to the lack of appropriate measurements. Another problem is the evaluation of measurement data from different sources (i.e. measuring techniques) for a special tyre, [2]. It is a known fact that different measuring techniques result in widely spread results. Here the experience of the user is needed to assemble a "probably best" set of data as a basis for the tyre model from these sets of data, and to verify it eventually with own experimental results.

Out of experience about the mentioned restrictions the followingly described tyre model TMeasy was conceived, which has proved successful in meeting practical requirements and which allows good correspondence between simulation and experiment. However, it should again be mentioned that a tyre model can only produce results of a quality according to the quality of the input data.

2 TMEASY: A TYRE MODEL "EASY TO USE"

2.1 Demands and Goals

An exact calculation of tyre forces is dependent on the knowledge of frictional behaviour between tyre and road. The coefficient of friction between rubber and asphalt, however, cannot be described in the simple form of a number. A large number of parameters influences, in mostly nonlinear form, the force transfer between a tread particle and the road surface. The most important factors of influence are the normal force and the sliding speed. Even if one succeeds in modelling the tyre in every detail, the problem of denominating the parameters for the law of friction remains.

Even the most complicated tyre model thus has to be, at least in respect to some model parameters, fitted to the results of measurements. Tyre models of such complexity however require a large calculation effort. They are usually used in basic studies.

In vehicle dynamics one usually applies the simpler semi-empirical tyre models. In these models, the tyre contact area is seen as an even plane and the tyre forces and torques are approximated by appropriate mathematical functions. The functions' parameters are set by adaption to measured tyre maps.

In vehicle dynamics, often the problem occurs that for a special type of tyre no or not all measurements are available. Questions pertaining the influence of aimed manipulations in the tyre behaviour, such as a larger increase of the tyre forces or a more or less distinct maximum, often occur. For that a tyre model is necessary that gives useful tyre forces from little information and in which the model parameters have concrete meaning.

The semi-empirical tyre model TMeasy has originally been conceived for vehicle dynamic calculations of agricultural tractors, [6]. Together with the software package Vedyna, it has proven successsful even for real time applications with cars, [1]. Recently it has been used for truck simulations with Simpack, [2].

2.2 Contact Point

The momentary position of the wheel with respect to the fixed x_0-, y_0-, z_0-system is defined by the wheel centre M and the unit vector e_{yR} in the direction of the wheel rotation axis, see Fig. 1.

On an uneven road, the contact point P cannot be calculated at once. Let point P^* with its horizontal coordinates x^*, y^* be a first estimation. Usually, P^* is not located on the road surface. The corresponding road point P_0 can be derived from the unevenness profile of the road $z = z(x^*, y^*)$.

At the point P_0 the road normal e_n is related to the tangential plane, determined by at least three points around the contact point P_0. The tyre camber angle γ describes the inclination of the wheel rotation axis e_{yR} against e_n. From e_n and e_{yR} the unit vectors in longitudinal e_x and lateral direction e_y can be easily calculated.
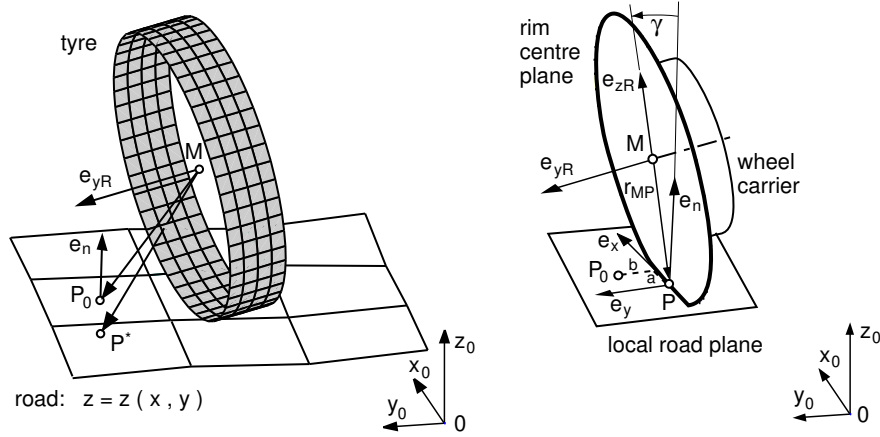
Figure 1: Contact Geometry

The vector from the rim centre M to the road point P_0 is now divided into three parts

$$r_{MP_0} = \underbrace{-r_S\, e_{zR}}_{r_{MP}} + a\, e_x + b\, e_y,$$ (1)

where r_S describes the static tyre radius, a, b state dislocations in longitudinal and lateral direction and the unit vector e_{zR} is perpendicular to e_x and e_{yR}. The contact point P, defined by the vector r_{MP} lies within the rim centre plane.

The shift from P_0 to P results according to Eq. (1) from parts $a\, e_x$ and $b\, e_y$, which are perpendicular to the road normal vector e_n. Because e_n has been calculated at the point P_0, on an uneven road P is not necessarily situated on the road surface. With $P^* = P$ as a new estimated value, the contact point P can be improved iteratively.

If the road is replaced by a plane in the tyre contact area, an iterative improvement is no longer necessary.

2.3 Dynamic Tyre Radius

Assuming that the tread particles stick to the road in the contact area, the jounced tyre moves at an rotation angle $\triangle\varphi$ along the distance x, Fig. 2.

If the movement of the tyre is compared with the rolling of a rigid wheel, the radius r_D has to be chosen in a way that at an rotation angle $\triangle\varphi$ the distance x is passed. As a first approximation, one gets

$$r_D = \frac{1}{3}\, r_0 + \frac{2}{3}\, r_S,$$ (2)

where r_0 is the undeflected and r_S is the deflected or static tyre radius. Due to $r_S = r_S(F_z)$ the fictive radius r_D depends on the wheel load F_z. Therefore it is called dynamic tyre radius.
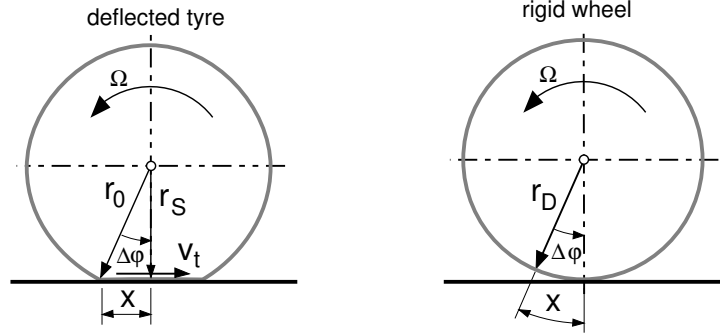
Figure 2: Dynamic Tyre Radius

If the tyre rotates at an rotational velocity Ω, then

$$v_t = r_D \, \Omega \qquad (3)$$

denotes the average velocity at which the tread particles are transported through the contact area.

2.4 Contact Point Velocities

The absolute velocity of the contact point P is given by

$$v_{0P} = v_{0M} + \triangle \dot{r} \, e_{zR} + \omega^*_{0WC} \times r_{MP} \,, \qquad (4)$$

where v_{0M} represents the velocity of the tyre centre M and $\triangle \dot{r}$ the change of the radial tyre deflection. Due to the rotational freedom between the wheel and its carrier, the effective angular velocity of the wheel carrier ω^*_{0WC} does not include any component in the direction of the wheel spin axis, i.e.

$$e_{yR}^T \, \omega^*_{0WC} = 0 \,. \qquad (5)$$

Because the point P is fixed to the road, Eq. (4) must not contain parts perpendicular to the local road plane. Hence, it holds

$$e_n^T \, v_{0P} = 0 \,. \qquad (6)$$

From this condition the wheel deformation velocity $\triangle \dot{r}$ can be calculated.

For the velocity parts in longitudinal and lateral direction one finally gets

$$v_x = e_x^T \, v_{0P} \quad \text{and} \quad v_y = e_y^T \, v_{0P}. \qquad (7)$$

2.5   Wheel Load

The vertical tyre force F_z can be calculated as a function of the normal tyre deflection $\triangle z = e_n^T \triangle z$ and the deflection velocity $\triangle \dot{z} = e_n^T \triangle \dot{r}$

$$F_z \;=\; F_z(\triangle z, \, \triangle \dot{z}) \,, \tag{8}$$

where the restriction $F_z \geq 0$ holds.

2.6   Longitudinal Force and Longitudinal Slip

The longitudinal slip

$$s_x \;=\; \frac{v_x - r_D \, \Omega}{r_D \, |\Omega|} \,. \tag{9}$$

is defined by the non-dimensional relation between the sliding velocity in longitudinal direction $v_x^G = v_x - r_D \, \Omega$ and the average transport velocity $r_D \, |\Omega|$.
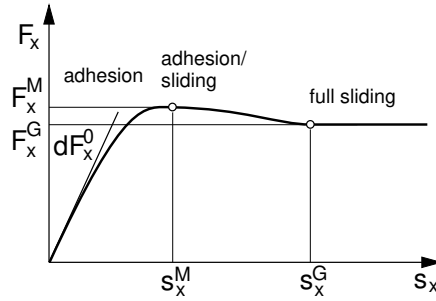

Figure 3: Typical Longitudinal Force Characteristics

The typical graph of the longitudinal force F_x as a function of the longitudinal slip s_x can be defined by the parameters initial inclination (longitudinal stiffness) dF_x^0, location s_x^M and magnitude of the maximum F_x^M, start of full sliding s_x^G and the sliding force F_x^G, Fig. 3.

Curves without peaks can be treated by setting the parameter maximum force F^M equal to the sliding force F^G. The remaining parameter s^M may be used for fitting the curve shape between the adhesion and the sliding region.

2.7   Lateral Slip, Lateral Force and Self Aligning Torque

Similar to the longitudinal slip s_x, Eq. (9), the lateral slip can be defined by

$$s_y \;=\; \frac{v_y^G}{r_D \, |\Omega|} \,, \tag{10}$$

where the sliding velocity in lateral direction is given by

$$v_y^G = v_y \tag{11}$$

and the lateral component of the contact point velocity v_y follows from Eq. (7).

As long as the tread particles stick to the road (small amounts of slip), an almost linear distribution of the forces along the contact area length L appears. At average slip values the particles at the end of the contact area start sliding, and at high slip values only the parts at the beginning of the contact area stick to the road, Fig. 4.
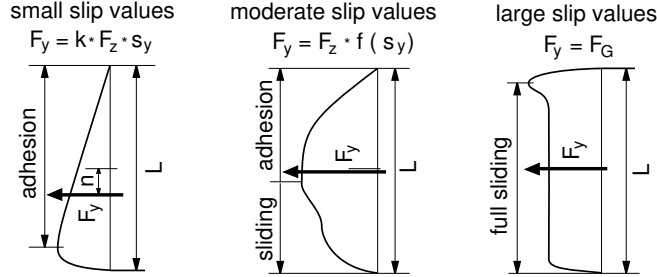

Figure 4: Principle of the Lateral Force Distribution at Different Slip Values

The distribution of the lateral forces over the contact area length also defines the acting point of the resulting lateral force. At small slip values the working point lies behind the centre of the contact area (contact point P). With rising slip values, it moves forward, sometimes even before the centre of the contact area. At extreme slip values, when practically all particles are sliding, the resulting force is applied at the centre of the contact area.

The resulting lateral force F_y with the dynamic tyre offset or pneumatic trail n as a lever generates the self aligning torque

$$M_S = -n \, F_y \, . \tag{12}$$

The lateral force F_y as well as the dynamic tyre offset are functions of the lateral slip s_y. Typical plots of these quantities are shown in Fig. 5. Characteristic parameters for the lateral force graph are initial inclination (cornering stiffness) dF_y^0, location s_y^M and magnitude of the maximum F_y^M, begin of full sliding s_y^G, and the sliding force F_y^G.

The dynamic tyre offset has been normalized by the length of the contact area L. The initial value $(n/L)_0$ as well as the slip values s_y^0 and s_y^G characterize the graph sufficiently.

2.8 Generalized Tyre Characteristics

The longitudinal force as a function of the longitudinal slip $F_x = F_x(s_x)$ and the lateral force depending on the lateral slip $F_y = F_y(s_y)$ can be defined by their characteristic parameters initial inclination dF_x^0, dF_y^0, location s_x^M, s_y^M and magnitude of the maximum F_x^M, F_y^M as well as sliding limit s_x^G, s_y^G and sliding force F_x^G, F_y^G, Fig. 6.
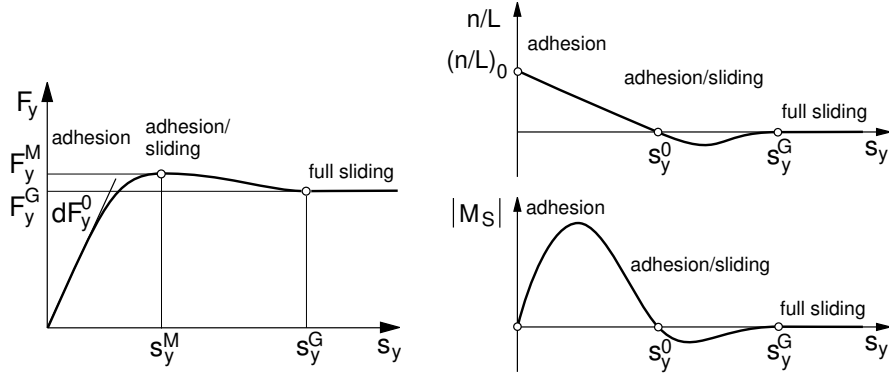
Figure 5: Typical Plot of Lateral Force, Tyre Offset and Self Aligning Torque

When experimental tyre values are missing, the model parameters can be pragmatically estimated by adjustment of the data of similar tyre types. Furthermore, due to their physical significance, the parameters can subsequently be improved by means of comparisons between the simulation and vehicle testing results as far as they are available.

During general driving situations, e.g. acceleration or deceleration in curves, longitudinal s_x and lateral slip s_y appear simultaneously. The combination of the more or less differing longitudinal and lateral tyre forces requires a normalization process, cf. [4], [3]. One way to perform the normalization is described in the following.

Generalized Slip

The longitudinal slip s_x and the lateral slip s_y can vectorally be added to a generalized slip

$$ s = \sqrt{\left(\frac{s_x}{\hat{s}_x}\right)^2 + \left(\frac{s_y}{\hat{s}_y}\right)^2}, \tag{13} $$

where the slips s_x and s_y were normalized in order to perform their similar weighting in s. For normalizing, the normation factors $\hat{s}_x$ and $\hat{s}_y$ are calculated from the location of the maxima s_x^M, s_y^M the maximum values F_x^M, F_y^M and the initial inclinations dF_x^0, dF_x^0.

Generalized Force

Similar to the graphs of the longitudinal and lateral forces the graph of the generalized tyre force is defined by the characteristic parameters dF^0, s^M, F^M, s^G and F^G. The parameters are calculated from the corresponding values of
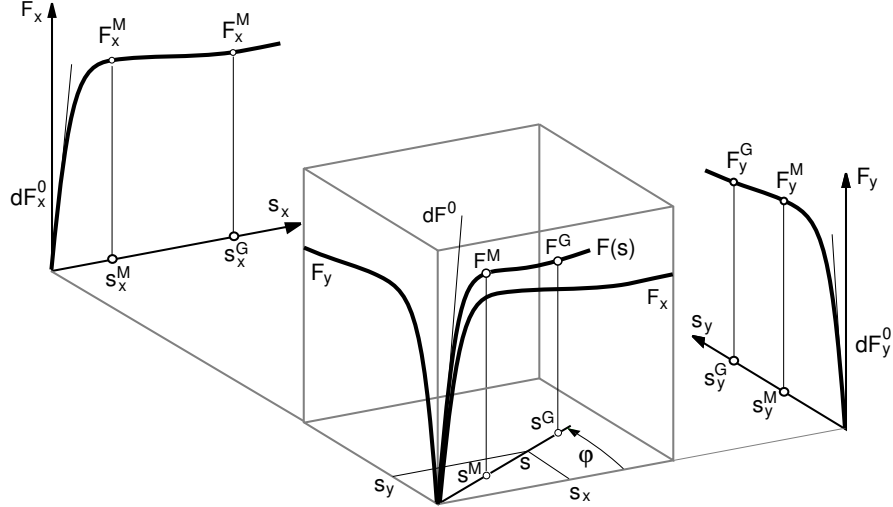
Figure 6: Generalized Tyre Characteristics

the longitudinal and lateral force

$$
\begin{aligned}
dF^0 &= \sqrt{\left(dF_x^0 \, \hat{s_x} \, \cos\varphi\right)^2 + \left(dF_y^0 \, \hat{s_y} \, \sin\varphi\right)^2}, \\
s^M &= \sqrt{\left(\frac{s_x^M}{\hat{s_x}} \, \cos\varphi\right)^2 + \left(\frac{s_y^M}{\hat{s_y}} \, \sin\varphi\right)^2}, \\
F^M &= \sqrt{\left(F_x^M \, \cos\varphi\right)^2 + \left(F_y^M \, \sin\varphi\right)^2}, \\
s^G &= \sqrt{\left(\frac{s_x^G}{\hat{s_x}} \, \cos\varphi\right)^2 + \left(\frac{s_y^G}{\hat{s_y}} \, \sin\varphi\right)^2}, \\
F^G &= \sqrt{\left(F_x^G \, \cos\varphi\right)^2 + \left(F_y^G \, \sin\varphi\right)^2},
\end{aligned}
\tag{14}
$$

where the slip normalization have also to be considered at the initial inclination. The angular functions

$$
\cos\varphi = \frac{s_x/\hat{s_x}}{s} \quad \text{and} \quad \sin\varphi = \frac{s_y/\hat{s_y}}{s}
\tag{15}
$$

grant a smooth transition from the characteristic curve of longitudinal to the curve of lateral forces in the range of $\varphi = 0$ to $\varphi = 90°$.

The function $F = F(s)$ is now described in intervals by a broken rational function, a cubic polynomial and a constant F^G

$$
F(s) = \begin{cases}
s^M \, dF^0 \, \dfrac{\sigma}{1 + \sigma \left(\sigma + F^0 \, \dfrac{s^M}{F^M} - 2 \right)} \,, & \sigma = \dfrac{s}{s^M} \,, & 0 \le s \le s^M \,; \\[4mm]
F^M - \left(F^M - F^G \right) \sigma^2 \left(3 - 2 \, \sigma \right) \,, & \sigma = \dfrac{s - s^M}{s^G - s^M} \,, & s^M < s \le s^G \,; \\[4mm]
F^G \,, & & s > s^G \,.
\end{cases}
$$

(16)

When defining the curve parameters, one just has to make sure that the condition $dF^0 \ge 2 \frac{F^M}{s^M}$ is fulfilled, because otherwise the function has a turning point in the interval $0 < s \le s^M$.

Longitudinal and lateral force now follow from the according projections in longitudinal and lateral direction

$$
F_x \;=\; F \, \cos\varphi \quad \text{and} \quad F_y \;=\; F \, \sin\varphi \,.
$$

(17)

Essential Parameters

The resistance of a real tyre against deformations has the effect that with increasing wheel load the distribution of pressure over the contact area becomes more and more uneven. The tread particles are deflected just as they are transported through the contact area. The pressure peak in the front of the contact area cannot be used, for these tread particles are far away from the adhesion limit because of their small deflection. In the rear of the contact area the pressure drop leads to a reduction of the maximally transmittable friction force. With rising imperfection of the pressure distribution over the contact area, the ability to transmit forces of friction between tyre and road lessens.

In practice, this leads to a degressive influence of the wheel load on the characteristic curves of longitudinal and lateral forces.

Longitudinal Force F_x		Lateral Force F_y	
$F_z = 3.2 \, kN$	$F_z = 6.4 \, kN$	$F_z = 3.2 \, kN$	$F_z = 6.4 \, kN$
$dF_x^0 \;=\; 90 \, kN$	$dF_x^0 \;=\; 160 \, kN$	$dF_y^0 \;=\; 70 \, kN$	$dF_y^0 \;=\; 100 \, kN$
$s_x^M \;=\; 0.090$	$s_x^M \;=\; 0.110$	$s_y^M \;=\; 0.180$	$s_y^M \;=\; 0.200$
$F_x^M \;=\; 3.30 \, kN$	$F_x^M \;=\; 6.50 \, kN$	$F_y^M \;=\; 3.10 \, kN$	$F_y^M \;=\; 5.40 \, kN$
$s_x^G \;=\; 0.400$	$s_x^G \;=\; 0.500$	$s_y^G \;=\; 0.600$	$s_y^G \;=\; 0.800$
$F_x^G \;=\; 3.20 \, kN$	$F_x^G \;=\; 6.00 \, kN$	$F_y^G \;=\; 3.10 \, kN$	$F_y^G \;=\; 5.30 \, kN$

Table 1: Characteristic Tyre Data with Degressive Friction Influence

In order to respect this fact in a tyre model, the characteristic data for two nominal wheel loads F_z^N and $2\,F_z^N$ are given in Tab. 1.

From this data the initial inclinations dF_x^0, dF_y^0, the maximal forces F_x^M, F_x^M and the sliding forces F_x^G, F_y^M for arbitrary wheel loads F_z are calculated by quadratic functions. For the maximum longitudinal force it reads as

$$F_x^M(F_z) = \frac{F_z}{F_z^N}\left[2\,F_x^M(F_z^N) - \tfrac{1}{2}F_x^M(2F_z^N) - \left(F_x^M(F_z^N) - \tfrac{1}{2}F_x^M(2F_z^N)\right)\frac{F_z}{F_z^N} \right].$$
(18)

The location of the maxima s_x^M, s_y^M, and the slip values, s_x^G, s_y^G, at which full sliding appears, are defined as linear functions of the wheel load F_z. For the location of the maximum longitudinal force this results in

$$s_x^M(F_z) = s_x^M(F_z^N) + \left(s_x^M(2F_z^N) - s_x^M(F_z^N)\right)\left(\frac{F_z}{F_z^N} - 1\right).$$
(19)

With the numeric values from Tab. 1 a slight shift of the maxima towards higher slip values is also modelled.

The bilateral influence of longitudinal s_x and lateral slip s_y on the longitudinal F_x and lateral force F_y is depicted in Fig. 7.

$$s_y = 0.0,\ 0.0375,\ 0.075,\ 0.1125,\ 0.15 \qquad s_x = 0.0,\ 0.0375,\ 0.075,\ 0.1125,\ 0.15$$

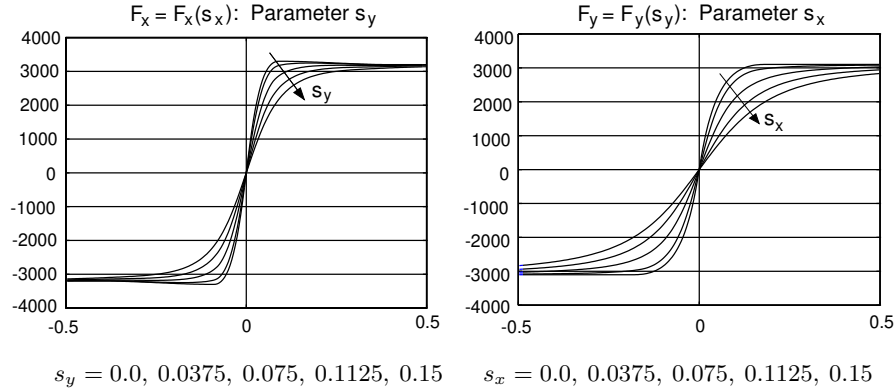Figure 7: Tyre Forces vs. Longitudinal and Lateral Slip: $F_z = 3.2\,kN$

With the 20 parameters, which are, according to Tab. 1, necessary for the definition of the characteristic curves of longitudinal and lateral force, the tyre model can be easily fitted to measured characteristics. Because for description of the characteristic curves of longitudinal and lateral force only characteristic curve parameters are used, a desired tyre behaviour can also be constructed in a convenient manner.

2.9   Camber Influence

If the wheel rotation axis is inclined against the road a lateral force appears, dependent on the inclination angle. At a non-vanishing camber angle, $\gamma \neq 0$ the

tread particles possess a lateral velocity when entering the contact area, which
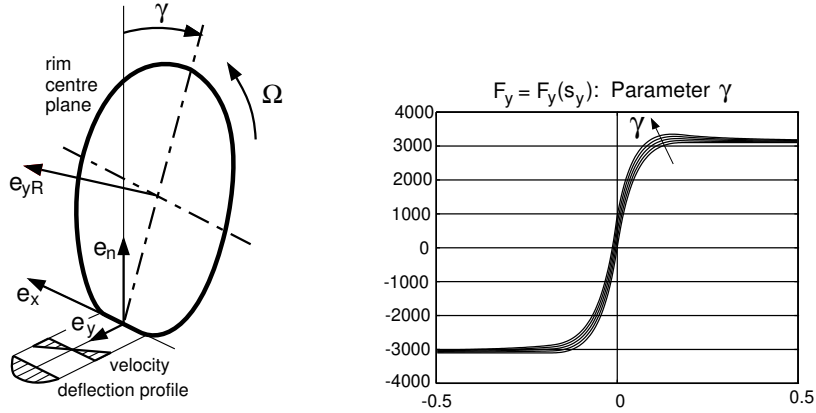is dependent on wheel rotation speed Ω and the camber angle γ, Fig. 8. At the

Figure 8: Cambered Tyre $F_y(\gamma)$ at $F_z = 3.2\,kN$ and $\gamma = 0°,\ 2°,\ 4°,\ 6°,\ 8°$

centre of the contact area (contact point) this component vanishes and at the
end of the contact area it is of the same value but opposing the component at
the beginning of the contact area. At normal friction and even distribution of
pressure in the longitudinal direction of the contact area one gets a parabolic
deflection profile, which is equal to the average deflection

$$\bar{y}_\gamma \;=\; \underbrace{\frac{L}{2}\,\frac{\Omega\,\sin\gamma}{R\,|\Omega|}}_{s_\gamma}\,\frac{1}{6}\,L \tag{20}$$

s_γ defines a camber-dependent lateral slip. A solely lateral tyre movement
without camber results in a linear deflexion profile with the average deflexion

$$\bar{y}_{v_y} \;=\; \underbrace{\frac{v_y}{R\,|\Omega|}}_{s_y}\,\frac{1}{2}\,L\ . \tag{21}$$

a comparison of Eq. (20) to Eq. (21) shows, that with $s_y^\gamma = \frac{1}{3}\,s_\gamma$ the lateral
camber slip s_γ can be converted to the equivalent lateral slip s_y^γ.

In normal driving operation, the camber angle and thus the lateral camber
slip are limited to small values. So the lateral camber force can be calculated
over the initial inclination of the characteristic curve of lateral forces

$$F_y^\gamma \;\approx\; dF_y^0\,s_y^\gamma\ . \tag{22}$$

If the "global" inclination $dF_y \approx F_y/s_y$ is used instead of the initial inclination
dF_y^0, one gets the camber influence on the lateral force as shown in Fig. 8.

The camber angle influences the distribution of pressure in the lateral direction of the contact area, and changes the shape of the contact area from rectangular to trapezoidal. It is thus extremely difficult if not impossible to quantify the camber influence with the aid of simple models. Therefore a plain approximation has been used, which still describes the camber influence rather exactly.

Due to the inclined rotation axis the cambered wheel also produces a bore velocity $\Omega_b = \Omega \sin\gamma$ which leads to the bore slip

$$s_b = \frac{\Omega \sin\gamma}{R\,|\Omega|}\,.\tag{23}$$

By a simple approach, c.f. [5], the resulting bore torque can be calculated from the characteristic tyre data.

2.10 Self Aligning Torque

According to Eq. (12) the self aligning torque can be calculated via the dynamic tyre offset.

The approximation as a function of the lateral slip is done by a line and a cubic polynome

$$\frac{n}{L} = \begin{cases} (n/L)_0\,(1 - |s_y|/s_Q^0) & |s_y| \le s_Q^0 \\[2ex] -(n/L)_0\,\dfrac{|s_y| - s_Q^0}{s_Q^0}\left(\dfrac{s_Q^E - |s_y|}{s_Q^E - s_Q^0}\right)^2 & s_Q^0 < |s_y| \le s_Q^E \\[2ex] 0 & |s_y| > s_Q^E \end{cases}\tag{24}$$

The cubic polynome reaches the sliding limit s_Q^E with a horizontal tangent and is continued with the value zero.

The characteristic curve parameters, which are used for the description of the dynamic tyre offset, are at first approximation not wheel load dependent. Similar to the description of the characteristic curves of longitudinal and lateral force, here also the parameters for single and double wheel load are given.

The calculation of the parameters of arbitrary wheel loads is done similar to Eq. (19) by linear inter- or extrapolation.

The value of $(n/L)_0$ can be estimated very well. At small values of lateral slip $s_y \approx 0$ one gets at first approximation a triangular distribution of lateral forces over the contact area length cf. Fig. 4. The working point of the resulting force (dynamic tyre offset) is then given by

$$n(F_z \to 0,\ s_y = 0) = \frac{1}{6}\,L\,.\tag{25}$$

The value $n = \frac{1}{6}\,L$ can only serve as reference point, for the uneven distribution of pressure in longitudinal direction of the contact area results in a change of the deflexion profile and the dynamic tyre offset.
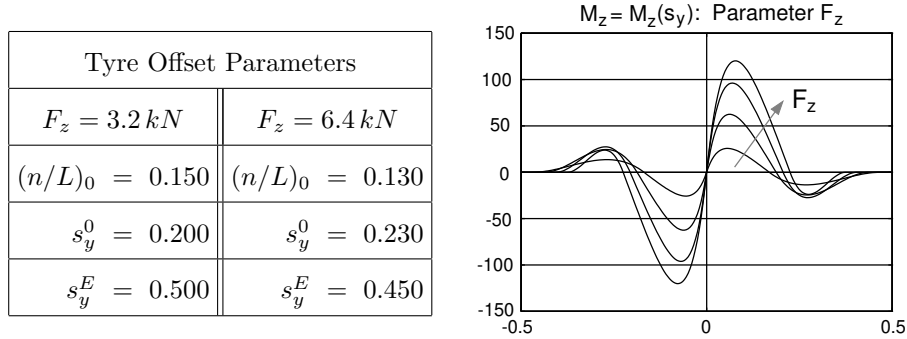
Tyre Offset Parameters	
$F_z = 3.2\,kN$	$F_z = 6.4\,kN$
$(n/L)_0 \;=\; 0.150$	$(n/L)_0 \;=\; 0.130$
$s_y^0 \;=\; 0.200$	$s_y^0 \;=\; 0.230$
$s_y^E \;=\; 0.500$	$s_y^E \;=\; 0.450$

Figure 9: Self Aligning Torque: $F_z = 0,\ 2,\ 4,\ 6,\ 8\,kN$

The self aligning torque in Fig. 9 has been calculated with the tyre parameters from Tab. 1, the tyre stiffness $c_R = 180\,kN/m$ and the undeflected tyre radius $r_0 = 0.293\,m$. The degressive influence of the wheel load on the lateral force can be seen here as well.

With the parameters for the description of the tyre offset it has been assumed that at double payload $F_z = 2\,F_z^N$ the related tyre offset reaches the value of $(n/L)_0 = 0.13$ at $s_y = 0$. Because for $F_z = 0$ the value $1/6 \approx 0.17$ can be assumed, a linear interpolation provides the value $(n/L)_0 = 0.15$ for $F_z = F_z^N$. The slip value s_y^0, at which the tyre offset passes the x-axis, has been estimated. Usually the value is somewhat higher than the position of the lateral force maximum. With rising wheel load it moves to higher values. The values for s_y^E are estimated too.

3   COMPARISON TO TEST RIG MEASUREMENTS

3.1   One-Dimensional Characteristics

The following comparison between simulation and experiment has been done with measurement data from the firms Continental and MAN, [2].

As one can see, Fig. 10, the characteristic curves $F_x = F_x(s_x)$, $F_y = F_y(\alpha)$ and $M_z = M_z(\alpha)$ are approximated quite well even for different wheel loads F_z. Obviously TMeasy is able to handle the different tyre types in a suitable manner. The "soft" truck tyre of type Radial 315/80 R22.5 at p=8.5 bar (right column) and the large differences between longitudinal and lateral force characteristics at the passenger car tyre of type Radial 205/50 R15, 6J at p=2.0 bar (left column) are represented without any considerable fitting problems.

The one-dimensional characteristics are automatically converted to a two-dimensional combination characteristics which are shown in Fig. 11.
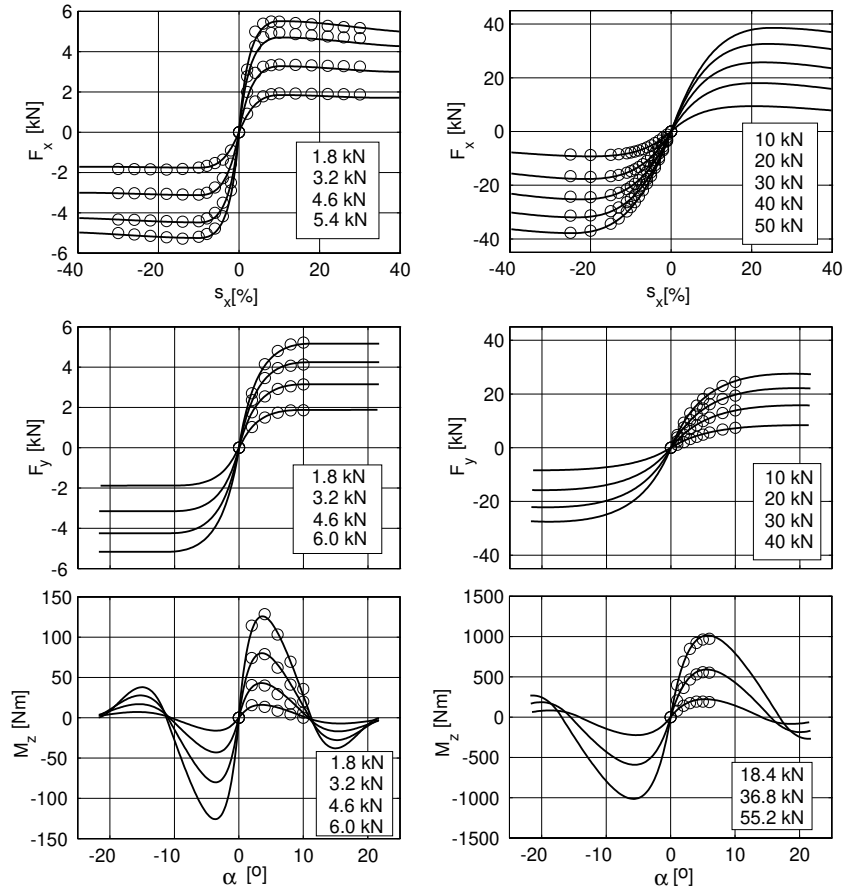
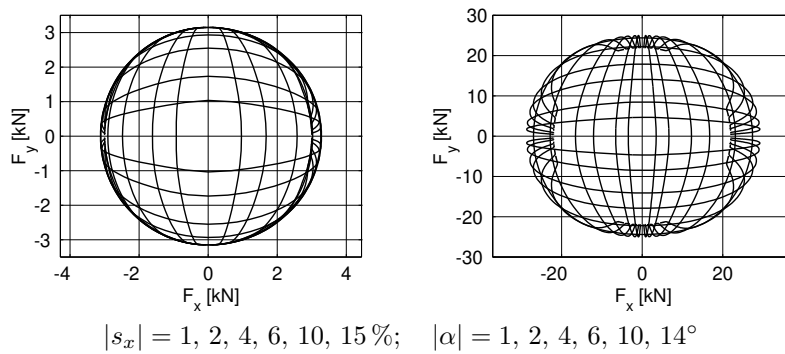Figure 10: Tyre Characteristics at Different Wheel Loads: ∘ Meas., − TMeasy

$$|s_x| = 1,\ 2,\ 4,\ 6,\ 10,\ 15\,\%; \quad |\alpha| = 1,\ 2,\ 4,\ 6,\ 10,\ 14°$$

Figure 11: Two-dimensional Tyre Characteristics at $F_z = 3.2\,kN$ / $F_z = 35\,kN$

3.2   Tyre Deflection and Dynamic Tyre Radius at zero camber

The static wheel load in TMeasy is described as a nonlinear function of the tyre deformation δ

$$F_z^S \;=\; a_1\,\delta \;+\; a_2\,\delta^2 \;. \tag{26}$$

The constants a_1 and a_2 are calculated from the radial stiffness at nominal payload

$$c_z^N \;=\; \left. \frac{d\,F_z^S}{d\,\delta} \right|_{F_z^S = F_z^N} \tag{27}$$

and the radial stiffness at double payload

$$c_z^{2N} \;=\; \left. \frac{d\,F_z^S}{d\,\delta} \right|_{F_z^S = 2F_z^N} \;. \tag{28}$$

In extension to Eq. (2), the dynamic tyre radius is approximated in TMeasy by

$$r_D \;=\; \lambda\,r_0 \;+\; (1-\lambda)\,\underbrace{\left(r_0 - \frac{F_z^N}{c_z^N} \right)}_{\approx\, r_S} \tag{29}$$

where the static tyre radius r_S has been approximated with the linearized tyre deformation F_z^N/c_z^N. The parameter λ is set as a function of the wheel load F_z

$$\lambda \;=\; \lambda_N \;+\; (\,\lambda_{2N} - \lambda_N\,) \left(\frac{F_z}{F_z^N} - 1 \right) \;, \tag{30}$$

where λ_N and λ_{2N} denote the values for the normal pay load $F_z = F_z^N$ and the doubled pay load $F_z = 2F_z^N$.
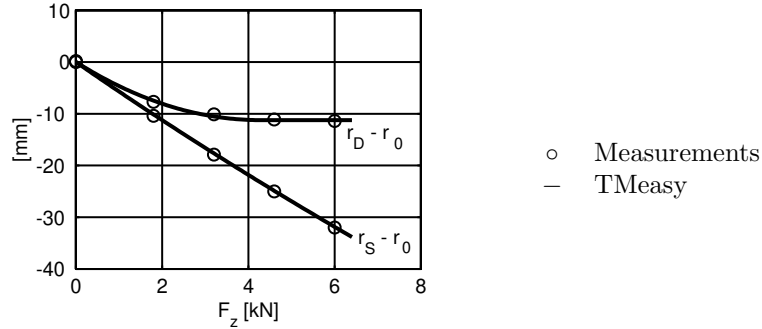

Figure 12: Tyre Deflection and Dynamic Tyre Radius Difference

With the TMeasy parameters for the passenger car tyre

```
vertical tyre stiffness at fz=fz0          [N/m],   190000.
vertical tyre stiffness at fz=2*fz0        [N/m],   206000.
```

```
coefficient for dynamic tyre radius fz=fz0   [-],    0.375
coefficient for dynamic tyre radius fz=2*fz0 [-],    0.750
```

the approximation of measured tyre data can be done very well, Fig. 12.

3.3 Tyre under Camber

TMeasy also takes the influence of a non vanishing tyre camber angle $\gamma \neq 0$ on the lateral force F_y and the self aligning torque M_z into account, Fig. 13.
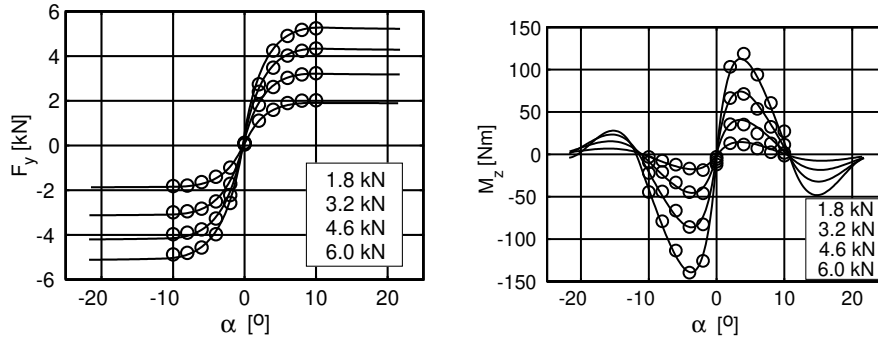

Figure 13: Lateral Force and Self Aligning Torque at $\gamma = 2°$ (car tyre)

Unfortunately, only experimental data for the car tyre were given. The asymmetric behaviour of the self aligning torque $M_z(-\alpha) \neq -M_z(\alpha)$ is mainly caused by the acting lateral velocity profile along the contact area while cambered, Fig. 8. As this part of tyre torque is modelled in TMeasy too, the measured self aligning torques are approximated very well.

4   IMPLEMENTATION AND APPLICATION

4.1 Interface

The implementation of TMeasy into a multi-body simulation system can easily be done over the Standard Tyre Interface (STI, [7]). This interface (current version 1.4) is supported today by many commercial simulation systems and allows the link of any STI-compatible tyre model, as far as they represent per definition vehicle dynamic models with an idealised contact point, cf. Fig. 14.

The simulation program passes the important wheel motion values in the sequence of wheels $W_i, i = 1, 2 \ ... \ n_W$ for every time interval to STI, which are here transformed into the internal motion values of the tyre models and are passed to it. As output, STI delivers the actual vectors of the tyre forces F_i and torques M_i in the specified form back to the simulation program. On necessity,
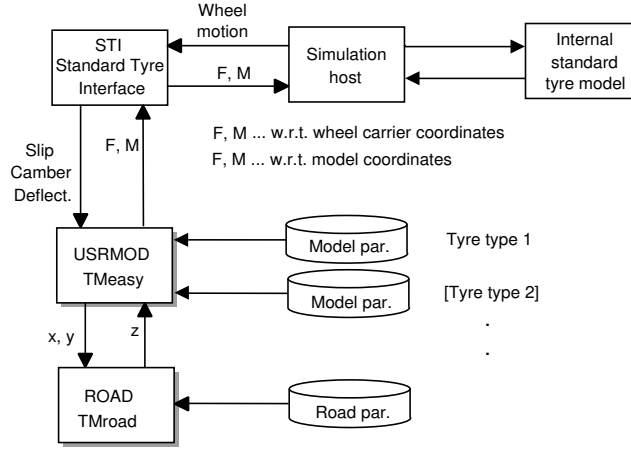
Figure 14: Implementation of TMeasy into a Simulation Program

from there they can be passed on to the according post processor for control purpose.

The coefficients of the chosen tyre types and the road parameters, e.g. geometry $z = z(x,y)$ and friction distribution $\mu = \mu(x,y)$ are provided over independent model data. A complete set of parameters for a vehicle model thus consists of at least one road file and one tyre file for each group of identical tyres, therefore, at least of one tyre file. The correct assignment of the tyre to its model body "wheel W_i" is defined in the model file and is directed by STI.

4.2   Application

The following example shows the results, chosen from [2], of a vehicle dynamic simulation of the standard driving maneuvre "double lane change" with a heavy truck-semitrailer combination on dry road, Tab. 2.

For this driving manoeuvre, experimental data exists; it is an important basis for the verification of the vehicle and tyre model during simulation. The multi-body model of the combination tractor-trailer is described in [2].

For the purpose of model verification, the steering angle gradient, which is recorded during the test run, is applied onto the vehicle model, while the measured driving velocity is regulated by a longitudinal controller. As vehicle dynamic comparative values the yaw velocities of tractor and trailer, the chassis-fixed lateral acceleration and the roll angle of the tractor are used.

The comparisons of simulation and experiments lead to the following comments, Fig 15:

Yaw rate and lateral acceleration: The simulation gives good comparative results. The deviations at maximum values rather refer to the experiment, as one can derive from the gradient of the other state variables. The achieved

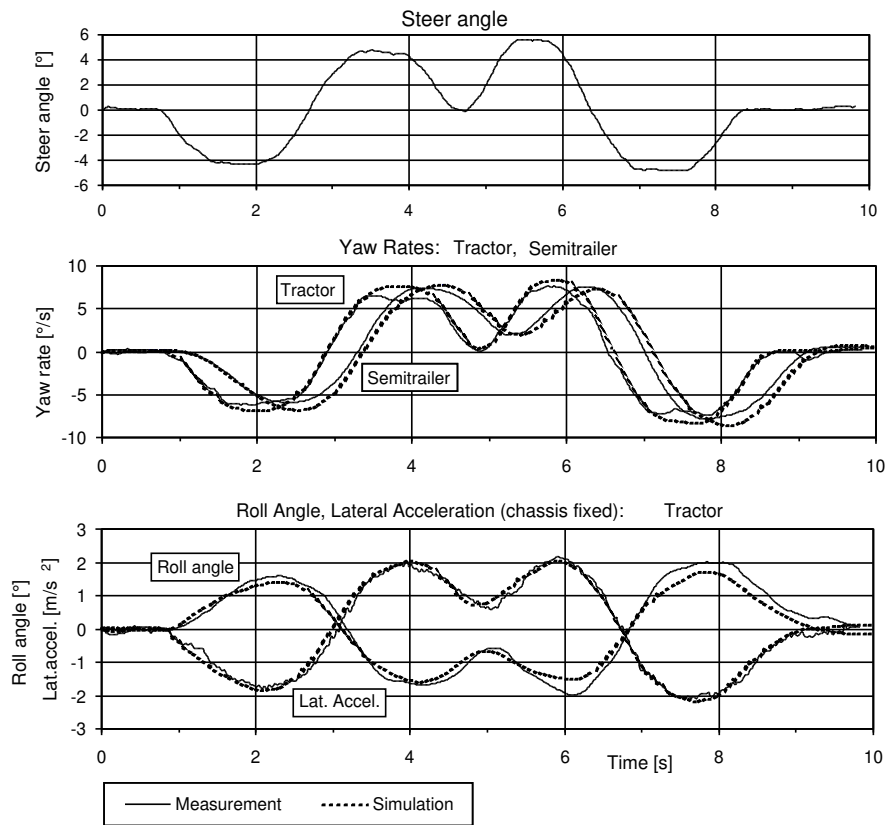| Vehicle:	MAN tractor-semitrailer combination, fully loaden: $m_G = 40\,t$		
Tyres:	Standard Radial Tyres:	front axle:	2 steering tyres,
		rear axle:	4 traction tyres,
		trailer axles:	6 trailer type tyres
Manoeuvre:	ISO Truck Lane Change on Dry Road.		
Simulation Package:	SIMPACK 8.0		
Tyre Model:	TMeasy 2.0		

Table 2: Technical Details

Figure 15: Double Lane Change at v = 60 km/h with a Fully Loaden Semitrailer

(vehicle fixed) lateral acceleration of $a_y = 2\,m/s^2$ grants a safe and roll-over stable driving state for the truck. The calculated yaw rate follows the measurement with short time delay.

Roll angle: Qualitatively experiment and simulation fit together very well, but the simulation gives little lower values for the rolling motion.

Figure 16: Animation of a Double Lane Change in the Limit Range

Finally, Fig. 16 shows the animation of the simulation result of a double lane change at high velocity, where the fully loaden vehicle combination comes close to the roll-over limit. Especially for examinations at vehicle dynamic stability limits, simulations with a verified vehicle and tyre model prove to be the risk-free alternative to investigate the active safety and to check the efficiency of the active control of steering, drive line and brakes. Even for that, the application of a certain and efficient tyre model is an important condition.

5   CONCLUSIONS

Forces and torques acting between the the tyres and the road surface are primarily responsible for a vehicle's dynamic behaviour, and particularly for its driving stability. There is an ever increasing interest in an accurate and efficient modelling of the tyre force reactions.

Due to their efficiency in computation and handling, the physically based, semi-empirical tyre models cover a wide range of practical demands in vehicle dynamics simulation. In particular, they allow at least sufficient approximations of the resulting force and torque characteristics, even in the case of incomplete

or missing measurement data. In contrast to that, pure formula based, empirical tyre models actually enable a high degree of modelling accuracy while requiring extensive sets of testing data in any case of application.

The present paper describes a physically based method called TMeasy, which is sufficiently simplified in order to get an analytical description of the acting tyre contact forces and torques. The tyre model's concept focuses on the practical requirements in vehicle dynamics analysis as one major aim. Typically, only a relative small number of model parameters has to be prepared. The direct physical meaning of these parameters should relieve the user in the fitting process. Thus, it is possible to offer a proper technical compromise between the modelling accuracy on the one hand and the user-friendliness on the other hand.

Furthermore, the idea of the described tyre model takes the dispersion of the related measurement data into account. It is a well known fact that for the same tyre type the results from different testing facilities disperse in a more or less considerable manner. In practice, often a pragmatical averaging is necessary.

As a further condition for practical applicability, the described tyre model is prepared to be linked to any multibody simulation system (MBS) which supports the Standard Tyre Interface (STI).

However, the model is restricted to steady state conditions at this moment. Concerning the prospects for further demands, it is intended to extend the tyre model TMeasy for the inclusion of the internal tyre dynamics under the particular aspect of practical requirements.

REFERENCES

1. Butz, T.: Parameter Identification in Vehicle Dynamics. Diplomarbeit, TU München, Zentrum Mathematik, München 1999.
2. Hirschberg, W., Weinfurter, H., Jung, Ch.: Ermittlung der Potenziale zur LKW-Stabilisierung durch Fahrdynamiksimulation. VDI-Berichte 1559 "Berechnung und Simulation im Fahrzeugbau" Würzburg, 14.-15. Sept. 2000.
3. Kortüm, W., Lugner, P.: Systemdynamik und Regelung von Fahrzeugen. Springer Verlag, Berlin 1993.
4. Pacejka, H.B., Bakker, E.: The Magic Formula Tyre Model. Proc. 1st Int. Colloquium on Tyre Models for Vehicle Dynamic Analysis, Swets&Zeitlinger, Lisse 1993.
5. Rill, G.: Simulation von Kraftfahrzeugen. Vieweg Verlag, Braunschweig 1994.
6. Rill, G., Salg, D., Wilks, E.: Improvement of Dynamic Wheel Loads and Ride Quality of Heavy Agricultural Tractors by Suspending Front Axles, in: Heavy Vehicles and Roads, Ed.: Cebon, D. and Mitchell C.G.B., Thomas Telford, London 1992.
7. Van Oosten, J.J.M. et al: Tydex Workshop: Standardisation of Data Exchange in Tyre Testing and Tyre Modelling. Proc. 2nd Int. Colloquium on Tyre Models for Vehicle Dynamic Analysis, Swets&Zeitlinger, Lisse 1997.